AGU PUBLICATIONS

Radio Science

RESEARCH ARTICLE
10.1002/2013RS005319

Special Section:
Green Radio Communications

Key Point:
- Channel models for body centric comms

Correspondence to:
S. L. Cotton,
simon.cotton@qub.ac.uk

Citation:
Cotton, S. L., R. D'Errico, and C. Oestges (2014), A review of radio channel models for body centric communications, *Radio Sci.*, *49*, doi:10.1002/2013RS005319.

Received 8 OCT 2013
Accepted 3 MAY 2014
Accepted article online 17 MAY 2014

This is an open access article under the terms of the Creative Commons Attribution-NonCommercial-NoDerivs License, which permits use and distribution in any medium, provided the original work is properly cited, the use is non-commercial and no modifications or adaptations are made.

# A review of radio channel models for body centric communications

**Simon L. Cotton[1], Raffaele D'Errico[2], and Claude Oestges[3]**

[1]ECIT Institute, Queen's University Belfast, Belfast, UK, [2]CEA, -LETI, Grenoble, France, [3]ICTEAM, Université catholique de Louvain, Louvain-la-Neuve, Belgium

**Abstract** The human body is an extremely challenging environment for the operation of wireless communications systems, not least because of the complex antenna-body electromagnetic interaction effects which can occur. This is further compounded by the impact of movement and the propagation characteristics of the local environment which all have an effect upon body centric communications channels. As the successful design of body area networks (BANs) and other types of body centric system is inextricably linked to a thorough understanding of these factors, the aim of this paper is to conduct a survey of the current state of the art in relation to propagation and channel models primarily for BANs but also considering other types of body centric communications. We initially discuss some of the standardization efforts performed by the Institute of Electrical and Electronics Engineers 802.15.6 task group before focusing on the two most popular types of technologies currently being considered for BANs, namely narrowband and Ultrawideband (UWB) communications. For narrowband communications the applicability of a generic path loss model is contended, before presenting some of the scenario specific models which have proven successful. The impacts of human body shadowing and small-scale fading are also presented alongside some of the most recent research into the Doppler and time dependencies of BANs. For UWB BAN communications, we again consider the path loss as well as empirical tap delay line models developed from a number of extensive channel measurement campaigns conducted by research institutions around the world. Ongoing efforts within collaborative projects such as Committee on Science and Technology Action IC1004 are also described. Finally, recent years have also seen significant developments in other areas of body centric communications such as off-body and body-to-body communications. We highlight some of the newest relevant research in these areas as well as discussing some of the advanced topics which are currently being addressed in the field of body centric communications.

## 1. Introduction

A body area network (BAN) is a self-contained wireless network in which constituent nodes are usually worn on or in close proximity to the human body. BANs are finding use in an increasing number of areas such as medical, military, sports and recreational applications. For example, a BAN used for medical purposes may employ nodes with in-built sensors to monitor life vitals such as heart rate, body temperature and gait with the aim of improving patient care. A typical BAN system can be based on star or star mesh hybrid topologies. In a star topology, the node data are always directly routed to a central node called a coordinator which again distributes the data to other nodes. In a star mesh hybrid topology, the node data can be directly routed to a destination node without being flowed through the coordinator (peer to peer link) i.e. all nodes can be used as relays [*Maman et al.*, 2009]. More generally dual-hop with different schemes have been proposed [*Chen et al.*, 2009] and proved to be efficient in the reduction of the packet error rate [*D'Errico et al.*, 2011; *Smith and Miniutti*, 2012].

Wireless links between BAN nodes operating within the popular Industrial Scientific and Medical (ISM) bands at 868/915 MHz, 2.45 and 5.8 GHz and surrounding frequencies, are often formed using on-body creeping waves [*Conway and Scanlon*, 2009; *Ryckaert et al.*, 2004; *Tsouri et al.*, 2011] and signal components reflected, diffracted, and scattered from other body parts [*Cotton et al.*, 2009b]. Depending upon the exact geometry of the wireless link, some BAN channels may also utilize free-space propagation (e.g., waist to wrist, etc.) as well as environmental multipath propagation whereby signal transmissions from an on-body node are returned toward the body from the local surroundings [*Cotton et al.*, 2009b; *Fort et al.*, 2007; *Hu et al.*, 2007]. Because nodes designed for BAN applications will be worn in close proximity to the human body, they will also be prone to antenna-body interaction effects, which include near-field coupling, radiation pattern


©2014. The Authors.

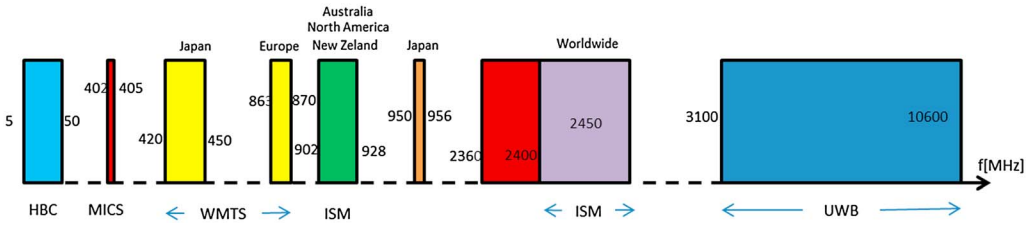


**Figure 1.** WBAN frequency bands allocated in different countries. Note that the UWB band is that defined by the Federal Communications Commission in the U.S.

distortion, and shifts in antenna impedance, which may degrade their efficiency and reduce signal reliability [*Conway et al*., 2008; *Conway and Scanlon*, 2009; *Giddens et al*., 2012; *Salonen et al*., 2004; *Sanz-Izquierdo et al*., 2006; *Wong and Lin*, 2005]. To complicate matters further, due to the inherent mobility, variations in body shape caused by movement and physiological processes such as respiration and also changes in the local environment, BAN channels are susceptible to time-varying, received signal characteristics [*D'Errico and Ouvry*, 2009; *Cotton et al*., 2009d; *Cotton and Scanlon*, 2009e].

Due to these complex electromagnetic interactions and changeable channel conditions, the design of physical (PHY) and medium access control (MAC) layer technologies to be used in body area networks present many challenges for wireless systems designers. This task is made even more difficult owing to the constraints placed on the size and power consumption of BAN nodes. In the PHY layer, nodes to be used in BANs are required to be compact, lightweight, robust, unobtrusive to the user, and usually feature antennas mounted conformal to or in extremely close proximity to the body surface. MAC layer protocols must be resilient to periods of outage triggered by shadowing of the link by the human body [*Alomainy et al*., 2007; *Van Torre et al*., 2012; *Wang et al*., 2009; *Rosini and D'Errico*, 2012a; *Cotton et al*., 2011]. These stringent requirements must be met, while still maintaining a high level of performance, reliability, and efficiency especially for niche and life critical applications in the medical and military domains [*Jovanov et al*., 2005; *Cotton et al*., 2009b].

The standardization of communications in BANs has largely been undertaken by the Institute of Electrical and Electronics Engineers (IEEE) 802.15 Task Group 6, also known as IEEE 802.15.6, which was setup in November 2007. The IEEE 802.15.6 standard [*IEEE*, 2012] appeared in February 2012 and defines the PHY and MAC layers optimized for short-range transmissions in, on or around the human body. Its purpose is to support low complexity, low cost, ultralow power, and highly reliable wireless communications for use in close proximity to, or inside, a human body (but not limited to humans) to serve a variety of applications both medical/healthcare and nonmedical related. The broad range of possible application fields in which BANs could be used, leads to an equally wide variety of system requirements that have to be met. The definition of a unique PHY layer has yet to yield a feasible solution. Hence, the IEEE 802.15.6 standardization group has proposed three different alternatives: a narrowband PHY centered at different frequencies, a UWB PHY, and a Human Body Communication PHY. Figure 1 graphically summarizes the spectrum allocation chart of all available frequencies for BAN applications, with the specification of the related country or region where they could be used.

As shown in Table 1, the standardization group has identified a list of scenarios in which IEEE 802.15.6 compliant devices will be expected to operate, along with their description and the frequency band of interest.

These scenarios were determined based on the physical positioning of the nodes and as a result, three different types of BAN node have been identified:

**Table 1.** List of Scenarios and Their Description

| Scenario | Description | Frequency Band | Channel Model |
|---|---|---|---|
| S1 | Implant to implant | 402–405 MHz | CM1 |
| S2 | Implant to body surface | 402–405 MHz | CM2 |
| S3 | Implant to external | 402–405 MHz | CM2 |
| S4 | Body surface to body surface (LOS) | 13.5, 50, 400, 600, 900 MHz 2.4, 3.1–10.6 GHz | CM3 |
| S5 | Body surface to body surface (NLOS) | 13.5, 50, 400, 600, 900 MHz 2.4, 3.1–10.6 GHz | CM3 |
| S6 | Body surface to external (LOS) | 900 MHz 2.4, 3.1–10.6 GHz | CM4 |
| S7 | Body surface to external (NLOS) | 900 MHz 2.4, 3.1–10.6 GHz | CM4 |


©2014. The Authors.

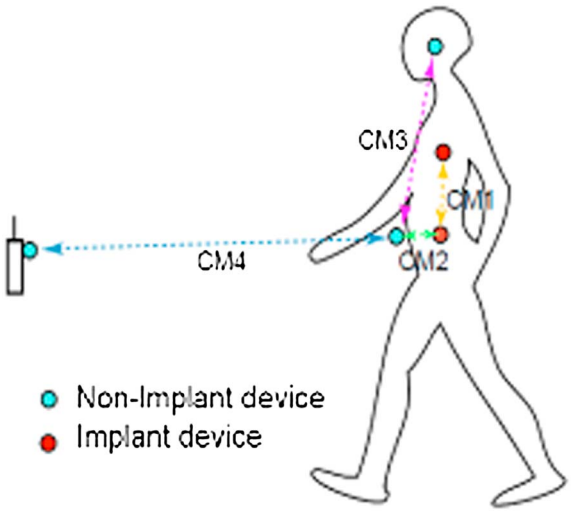


**Figure 2.** IEEE Channel models [*Yazdandoost and Sayrafian-Pour*, 2010].

1. *Implant node*: placed inside the human body, immediately below the skin or deeper inside the body tissue.
2. *Body surface node*: placed on the surface of the human skin or at most 2 cm away.
3. *External node*: not in contact with human skin (between a few centimeters and up to 5 m away from the body).

In Table 1, the scenarios are grouped into classes that can be represented by the same Channel Model (CM). It is important to remark that the channel model for scenarios involving implanted devices is fundamentally different from the one characterizing body surface communications. For that reason, the CMs are divided into two subgroups: CM1 and CM2 for channel models involving at least one implant device and CM3 along with CM4 for the body surface to body surface or to external node communications. A graphical representation of the scenarios and the relative channel model is presented in Figure 2. In this paper, we focus on the PHY layer link characteristics and in particular the current state of art in relation to channel modeling for BANs considering body surface-to-body surface communications. We will also consider off-body communications (CM4) as well as emerging body-to-body communications channels.

## 2. Narrowband Channel Models

Given the large number of variable parameters responsible for shaping the characteristics of the wireless channel for BAN applications, it is often easier to analyze these channels using statistics, where given a particular scenario, a probability level is assigned to a channel output parameter such as the received signal or phase. To further simplify the analysis, BAN channels are often studied in various environments with specific user actions considered separately (e.g., standing in a hallway, walking in an open office area, running outdoors, etc.). These results may be either reported in isolation or where applicable, aggregated to create more generic BAN channel models. In most cases, this will allow the on-body channel statistics to be considered as wide sense stationary, that is, the first and second moments do not vary with respect to time.

As discussed earlier, there are a number of different frequency bands of interest for BAN applications, e.g., the MICS bands and ISM bands. In the IEEE 802.15.6 standard different narrowband PHYs are proposed: 402–405 MHz, 420–450 MHz, 863–870 MHz, 902–928 MHz, 950–958 MHz, 2.36–2.4 GHz, and 2.4–2.4835 GHz (see *Smith et al.* [2013, Table 1] for further information). However, most of the work on channel modeling presented in literature has focused on 868 MHz and particularly the worldwide 2.4 GHz bands, since the radio technology is already or partially available in the market. As a consequence this section is focused on the channel modeling in these bands, addressing the main studies on path loss as well as first- and second-order statistics.

### 2.1. Path Loss Models

Due to the geometry of the human body and the multitude of different signal path trajectories which are possible, it can be quite difficult to fit a general distance related path loss model to the data obtained in on-body channels. For example, consider an on-body link that traverses (in line of sight) from the front right chest to the front right waist, now consider a link of the same length from the front right waist to somewhere along the waist on the posterior side of the body. This link, despite having the same length (when measured along the perimeter of the body surface), is nonline of sight (NLOS) and thus subject to very different propagation mechanisms and hence likely to experience much greater attenuation. This inability to apply a one-model-fits-all approach has led to the conclusion [*D'Errico and Ouvry*, 2009; *Smith et al.*, 2009b, 2013] that path loss models are inappropriate for BAN communications. Despite this, there has been some investigation of path loss models for BAN channels for very well defined scenarios and links. For example, in [*Roelens et al.*, 2006], an empirical path loss model based on the Friis formula in free space for on-body


©2014. The Authors.

**Table 2.** CM3A Model Parameters

| Parameter | Hospital Room | Anechoic Chamber |
|---|---|---|
| a | 6.60 | 29.3 |
| b | 36.1 | −16.8 |
| $\sigma_N$ | 3.80 | 6.89 |

communication at 2.4 GHz was presented and shown to provide a good fit to measured and simulated data for transmitter-receiver separations up to 40 cm. The authors considered a flat, lossy medium, representing human tissue and characterized the relationship between the antenna height above human tissue and model parameters such as the path loss exponent and the path loss at the chosen reference distance. In *Reusens et al*. [2007], the path loss based on the Friis formula was again considered. In this study, path loss along the torso and along the arm were measured and while the path loss exponent, $n$, for propagation along both media were almost the same ($n \approx 3.3$), the path loss along the torso was higher than the arm. The authors reasoned that this effect may have been due to much greater absorption in the torso and its geometry being much less flat than the stretched arm.

In the IEEE 802.15.6 channel model [*Yazdandoost and Sayrafian-Pour*, 2010; *IEEE*, 2012], the conventional approach for modeling the path loss, precisely as a function of the distance $P(d)$, was used, although it is questionable due to the phenomenon discussed above whereby on-body signal paths with the same length can be subject to very different propagation mechanisms and thus large differences in path loss. Nonetheless, a power law model, namely, CM3A in the IEEE 802.15.6 document, was presented as follows:

$$P_{dB}\left(d_{[mm]}\right) = a \cdot \log\left(d_{[mm]}\right) + b + N \tag{1}$$

where $a$ and $b$ are parameters of the model and $N$ is a normally distributed variable, centered, and with standard deviation $\sigma_N$ (see Table 2) and $d$ is the transmitter-receiver separation in this instance, expressed in millimeters. Note that the parameter values given in Table 2 were abstracted from measurements made in the 2.4–2.5 GHz band. Details of the measurement set up, derivation and data analysis can be found in *Aoyagi et al*. [2008].

A saturation model has been also presented in *Yazdandoost and Sayrafian-Pour* [2010]. This kind of model is "hybrid" in the sense that it merges a local propagation model (on-body to on-body, or "on-on") and the influence of the environment (typically multipath components—MPCs—reflecting off of the walls) resulting in an exponential part for "short distances" (on-on mechanism) and a "saturation" for larger distances. It has been proposed for narrowband channels at 915 MHz and 2.4 GHz. The corresponding formula (which was proposed by *Fort et al*. [2007] and used in the Table 8.2.5.B and Table 8.2.6.C of *Yazdandoost and Sayrafian-Pour* [2010]) is given by

$$P_{\mathrm{dB}}\left(d_{[\mathrm{cm}]}\right) = -10 \cdot \log_{10}\left(P_0 e^{-m_0 d_{[cm]}} + P_1\right) + \sigma_p n_p \tag{2}$$

In this model, $P_{\mathrm{dB}}$ represents the path loss in decibels at a distance $d$ measured around the body in centimeters. Physically, $P_0$ depends on the average losses occurring close to the transmitter and will depend on the kind of antenna. $P_1$ is the average attenuation of components in an indoor environment radiated away from the body and reflected back toward the receiving antenna. The parameter $m_0$ represents the average exponential decay rate in dB/cm of the creeping wave component diffracting around the body; $n_p$ is a zero mean and unit variance Gaussian random variable, and $\sigma_p$ is the lognormal variance in dB around the mean, representing the variations measured at different body and room locations. This parameter will depend on variations in the body curvature, tissue properties, and antenna radiation properties at different body locations. This model, namely, CM3B, is based on measurements conducted at 2.45 GHz. Details of the measurement setup, derivation, and data analysis can be found in *Dolmans and Fort* [2008]. The path loss follows an exponential decay around the perimeter of the body. It flattens out for large distances due to the contribution of MPCs from the indoor environment. Table 3 presents the model and the corresponding parameters.

**Table 3.** CM3B Model Parameters

| Parameter | Value |
|---|---|
| $P_0$[dB] | −25.8 |
| $m_0$[dB/cm] | 2.0 |
| $P_1$[dB] | −71.3 |
| $\sigma_p$[dB] | 3.6 |

As part of the IEEE 802.15.6 channel modeling efforts, scenario-dependent models have also been developed where the path loss is obtained from measurements averaging sources of variability (e.g., differing human subjects, and/or "local positioning", posture, unwanted movements, antennas, etc.). Path loss measurements were performed at a frequency of 2.36 GHz for everyday activities such as standing, walking, and running within an indoor environment.


©2014. The Authors.

**Table 4.** CM3C Model Parameter

| | Receiver at Right Hip | | | | | | Receiver at Chest | | |
|---|---|---|---|---|---|---|---|---|---|
| Action | Chest | Right Wrist | Left Wrist | Right Ankle | Left Ankle | Back | Back | Right Wrist | Right Ankle |
| Standing | 65.3 | 44.5 | 74.7 | 60.9 | 70.7 | 75.3 | 73 | 70.5 | 66.3 |
| Walking | 59.1 | 47.3 | 59.8 | 53.9 | 58.5 | 67.4 | 72 | 64.9 | 62.4 |
| Running | 55.9 | 36.3 | 52.5 | 55.0 | 59.0 | 68.5 | 71.7 | 57.4 | 63.3 |

An exact description of the measurement setup, derivation, and data analysis can be found in *Miniutti et al.* [2008]. The path loss model considered for this study had the form

$$P_{\mathrm{dB}} = P_{Tx} - P_{Rx} + G_{\mathrm{amplifier}} - L_{\mathrm{cable}} \tag{3}$$

where $P_{Tx}$ represents the transmitted power, i.e., incident on the transmitting antenna port, $P_{Rx}$ the RMS received power, i.e., incident on the receiving antenna port, $G_{\mathrm{amplifier}}$, the amplifier gain and $L_{\mathrm{cable}}$, the cable loss, used in the test bed. Table 4 presents the results of fitting equation (3) to the experimental data obtained in this study, i.e., the average path loss $P_{\mathrm{dB}}$.

Analytical models based on electromagnetic theory have also been applied to the study of signal attenuation on human tissue [*Conway et al.*, 2010; *Chandra and Johansson*, 2013]. In *Conway et al.* [2010], analytical models for the calculation of the approximate path gain, both along and around planar and cylindrical geometries at 2.45 GHz were verified using measurements and finite difference time domain (FDTD) simulation. The results obtained show that along the body surface (planar) transmission has a decay index of $n \approx 2.4$–$2.5$. However, the increased diffraction losses and nonline of sight conditions for around the body links gives a much higher decay index of $n \approx 4.0$–$4.5$. In *Chandra and Johansson* [2013], Chandra and Johansson proposed a much more realistic analytical model of on-body wave propagation based on creeping wave propagation over an elliptical approximation of the human which also includes the influence of the arms. Using electromagnetic simulations based on FDTD, they were able to show that the link loss can be underestimated by as much as 16 dB when the arms are omitted from the model.

Ryckaert et al. [*Ryckaert et al.*, 2004] take a different approach than the studies listed above and modeled the path loss around the human body as a function of the angle between transmitting and receiving antennas. Performing simulations at 400 MHz, 900 MHz, and 2.4 GHz using the FDTD technique, signal propagation around the human body was analyzed at eight different elevations along the human body. For each slice, the field emanating from a dipole antenna placed at the front of the body was evaluated at 15 radial points following the shape of the body. It was found that from a certain angle on, the propagation around the human body turns into an interference regime. The creeping wave that turned clockwise starts to interfere with the one that turned anticlockwise. In the interference region, the decay is smaller but the variability of the field is much larger. The width of the zone depends on the relative strength and on the wavelength of the creeping waves. The dual-slope path loss model proposed in *Ryckaert et al.* [2004] is expressed as

$$\begin{aligned} P_{\mathrm{dB}}(\theta) &= P_{\mathrm{dB}}(\theta_0) - \gamma_1(\theta - \theta_0) && \text{for } \theta_0 < \theta \le \theta_{bp} \\ P_{\mathrm{dB}}(\theta) &= P_{\mathrm{dB}}(\theta_{bp}) - \gamma_2(\theta - \theta_{bp}) && \text{for } \theta_{bp} < \theta \le \pi \end{aligned} \tag{4}$$

where $\gamma_i$ and $\theta_{bp}$ are the decay coefficient and break point angle, respectively.

### 2.2. Fading Statistics

As discussed above, if we initially ignore multipath generated by the local surroundings, the fading observed in on-body communications channels is typically the result of body shadowing and small-scale fading generated by the human body. When operating in reverberant environments, multipath generated by the local surroundings becomes an important factor in BAN channels and cannot be ignored [*Cotton et al.*, 2009b]. Body shadowing occurs in BAN channels when the signal path between the transmitting and receiving nodes is obscured by human tissue and moving limbs. Its magnitude will depend on the differing size and (dielectric) constitution of the human tissue obscuring the on-body link [*Oliveira and Correia*, 2010]. It is considered by many researchers to be one of the most predominant factors when determining on-body channel characteristics [*Alomainy et al.*, 2007; *Boulis et al.*, 2012]. The authors of *Boulis et al.* [2012] have performed a wide variety of dynamic channel measurements of "everyday" activities such as walking, running, driving, at the office, at home, outdoors, and sleeping. The measurements were conducted near the 900 and


©2014. The Authors.

2400 MHz ISM bands and totaled many hundreds of hours, mainly using bespoke bodyworn nodes. They have shown that the attenuation in on-body channels, predominantly due to shadowing, can be significantly large, with median channel attenuation greater than 70 dB. For measurements conducted in an anechoic chamber, and therefore excluding environmental multipath, Alomainy *et al.* [*Alomainy et al.*, 2007] have measured the wireless link between two microstrip patch antennas mounted on the human body. The attenuation attributed to factors such as the body, head, and clothing were found to be 19.2, 13.0, and 1.7 dB, respectively. The problem of body shadowing is particularly prevalent for emerging millimeter-wave on-body communications at 60 GHz [*Chahat et al.*, 2013], where it is postulated that the significant shadowing effect from the human body is expected to make NLOS communications very difficult, if not impossible.

#### 2.2.1. First-Order Statistics

To abstract the signal component due to body shadowing, the received signal is often filtered or "demeaned" using an appropriate window size [*Liu et al.*, 2011; *Cotton and Scanlon*, 2006; *D'Errico and Ouvry*, 2010a; *Rosini and D'Errico*, 2012a]. The size of the window is often directly related to the BAN link and the user's actions. For example, in *D'Errico and Ouvry* [2010a] the authors made a range of on-body channel measurements at 2.45 GHz covering the left hip to the chest, right thigh, right wrist, and right foot and left ear to right ear, hip, right wrist, and right foot in both an anechoic and indoor environments. They used a sliding temporal window of 10 channel samples, or equivalently 200 ms for their measurement setup, to remove the fading due to body shadowing from the received signal. In this study, it was found that distribution of the body shadowing component was well described by the lognormal distribution or equivalently the normal distribution when the body shadowing signal is subject to a logarithmic transform. The authors also found that the shadowing strictly depends on the movement type and the human body. More specifically, when the subject does not move the impact of body shadowing is moderate; however, when the subject moves, the degree of shadowing increases, becoming dependent on the way each human subject moves and the path trajectory.

To model the small-scale fading component in these studies [*Liu et al.*, 2011; *Cotton and Scanlon*, 2006; *D'Errico and Ouvry*, 2010a; *Rosini and D'Errico*, 2012a], the Rice $K$ factor has been used. The Rice $K$ factor [*Stüber*, 2011] is defined as the ratio of the square of the dominant component ($c^2$) to the scattered power ($2s^2$), i.e., $K = c^2/2s^2$. When $K \to 0$, and hence the dominant component $c$ decreases, the fading becomes closer to Rayleigh fading, and as $K \to \infty$, the channel no longer exhibits fading. In *Cotton and Scanlon* [2006] and *D'Errico and Ouvry* [2010a] it was observed that when the human subject was stationary, the estimated $K$ factors for on-body communications channels are large, e.g., $K = 316$ for the right chest to back left at 868 MHz while human subject was stationary in anechoic chamber [*Cotton and Scanlon*, 2006], as there was very little small-scale fading. In contrast, when the human subject becomes mobile, $K$ factors are observed to decrease especially within indoor environments, were signal components returned toward the body from the local surroundings act to increase the scattered power in on-body channels ($K = 1.82$ for the same channel in *Cotton and Scanlon* [2006] while the human subject was mobile in an open office environment). It has also been reported that the magnitude of the $K$ factor also changes with time [*Nechayev et al.*, 2009]. In this study, on-body channel characteristics were monitored over a wide range of everyday environments as a test subject performed various activities such as driving a car, walking outdoors and indoors, and sitting.

Rather than decompose the received signal into body shadowing and small-scale components, many studies have characterized the received signal in on-body channel as a single random variable. Popular fading models have included lognormal [*Cotton and Scanlon*, 2007a, 2009a; *Chaganti et al.*, 2010], Rayleigh [*Fort et al.*, 2007], Rice [*Fort et al.*, 2007], Nakagami-*m* [*Cotton and Scanlon*, 2009a; *Kim and Takada*, 2009], and Weibull [*Smith et al.*, 2009a; *Kim and Takada*, 2009]. The lognormal PDF for an envelope $R$ with mean $\xi$ and standard deviation $\beta$ may be expressed as [*Cotton and Scanlon*, 2007a]

$$f_R(r) = \frac{1}{r\beta\sqrt{2\pi}} \exp\left(-\frac{[\ln(r) - \xi]^2}{2\beta}\right) \tag{5}$$

where $r > 0$. Lognormal random variables can be viewed as the result of a number of multiplicative factors that become additive under logarithmic transformation. A physical interpretation of lognormal fading in on-body channels has been proposed in *Fort et al.* [2006], where the received signal is the result of diffraction, reflection, energy absorption, and antenna losses. Lognormal fading has been reported for on-body


©2014. The Authors.

communications channels at 2.45 GHz when the test subject was both stationary [*Cotton et al*., 2009b] and performed routine activities including walking around the office, using the restroom, getting coffee, and working at their desk [*Chaganti et al*., 2010].

In Rayleigh fading, the received signal is viewed as the resultant of a large number of scattered signal components, each with random amplitude and uniform phase. Rayleigh fading has been reported for on-body links where communications occur around the human torso at both 915 MHz and 2.45 GHz [*Fort et al*., 2007]. It is rationalized that diffracting components which travel distances greater than 35 cm, around the back of the body become significantly attenuated. Instead, the received signal is made up of reflected components, which follow a Rayleigh distribution. In on-body channels, where a line of sight (LOS), strong on-body reflection, or dominant creeping wave component exists, it may be more appropriate to model the distribution of received signal as following a Rice probability density function (PDF). The PDF of a Rice distributed random variable, $R$, may be written as [*Rice*, 1948]

$$f_R(r) = \frac{r}{s^2}\exp\left(-\frac{(r^2+c^2)}{2s^2}\right) I_0\left(\frac{rc}{s^2}\right), \quad r \geq 0 \tag{6}$$

In the absence of a dominant component (i.e., $c = 0$), the Rice PDF becomes equivalent to the Rayleigh PDF. Ricean fading was reported in *Fort et al*. [2007] for on-body link distances less than 25 cm; it was observed that as the separation distance of the on-body link increases, the $K$ factor decreases (as defined above), due to greater attenuation of the creeping wave component.

Nakagami-$m$ fading has been reported in a number of studies characterizing BAN channels. The PDF of a Nakagami fading signal envelope is given by *Yacoub et al*. [1999]

$$f_R(r) = \frac{2m^m r^{2m-1}}{\Gamma(m)\Omega^m}\exp\left(-\frac{mr^2}{\Omega}\right), \quad r \geq 0 \tag{7}$$

where $m = \mathrm{E}^2(R^2)/\mathrm{var}(R^2)$ and $\Omega = \mathrm{E}(R^2)$. Nakagami-$m$ random variables may be generated as the sum of $m$ independent and identically distributed Rayleigh components with mean power $\Omega$/m [*Filho and Yacoub*, 2009]. Like the Rice PDF, the Rayleigh PDF also appears as a special case of the Nakagami-$m$ PDF when $m = 1$. The Nakagami-$m$ distribution has the added advantage over the Rayleigh and Rice PDFs in that it can model fading which is worse than Rayleigh, i.e., $m < 1$ [*Yacoub et al*., 1999]. In *Cotton et al*. [2009b], for BAN channel measurements made at 2.45 GHz considering wireless nodes distributed across the body, covering the head, upper front and back torso, and the limbs, it was observed that when the test subject was stationary, Nakagami-$m$ parameters were always much larger than 1, irrespective of the operating environment. In an anechoic environment, when the user became mobile, the measured Nakagami-$m$ parameters were observed to decrease due to an increase in the diffuse contributions from the body and interruption of the on-body creeping wave component (if present). Similar to the Rice $K$ factors reported in reference [*Fort et al*., 2007], the Nakagami-$m$ parameter was typically observed to decrease with increasing separation distance between on-body antennas. Fading in on-body channels was also observed to increase when the user moved into a multipath environment, showing that the local surroundings are an important consideration for on-body systems. For on-body links operating at 4.5 GHz [*Kim and Takada*, 2009], Nakagami-$m$ fading has also been found to occur for scenarios when the test subject performed walking movements in an anechoic chamber.

In a Weibull fading channel, the received signal is obtained as a nonlinear function of the modulus of multipath components, where the nonlinearity is expressed in terms of the power parameter $\alpha$. The PDF of a Weibull distributed envelope may be written as [*Yacoub et al*., 2005]

$$f_R(r) = \frac{\alpha r^{\alpha-1}}{\lambda}\exp\left(-\frac{r^\alpha}{\lambda}\right) \tag{8}$$

where $\lambda = \mathrm{E}^2(R^\alpha)$. Again, identical to the Rice and Nakagami-$m$ distributions, the Rayleigh distribution may be obtained from the Weibull distribution by setting $\alpha = 2$ [*Yacoub*, 2007]. Weibull fading has been reported for on-body measurements made at 2.36 GHz while the test subject was walking and running [*Smith et al*., 2009a] and at 4.5 GHz for walking and standing up/sitting down motions [*Kim and Takada*, 2009]. In *Kim and Takada* [2009], it is suggested that the Weibull model should be used for on-body links which experience severe fading such as the shoulder and ankle, while the user was walking, and the entire trunk area, while the user was repeating standing up/sitting down motions.


©2014. The Authors.

In addition to using popular statistical distributions parameterized by measurements, the fading behavior of on-body channels in a specific scenario was investigated in *Liu et al*. [2011] by means of a physical-statistical approach. A general full-wave solution of a polarized point or line source with multiple cylinder scattering was developed, considering that the source is located on the trunk and modeling the shapes of the trunk and arms as three infinite cylinders. By allowing the arms to swing periodically along the main cylinder, the lognormal fading statistics encountered during a typical walk can be reproduced. The advantage of the method is that the second-order statistics are inherently included in the model as a function of the arm swinging pattern. More details on these results are provided in the next section.

#### 2.2.2. Doppler and Time Dependencies

Recent years have seen a sustained effort to improve our understanding of how to model the Doppler and time dependencies in BAN channels [*Cotton et al*., 2013; *Cotton and Scanlon*, 2009c; *Cotton et al*., 2009f; *Smith et al*., 2009a; *Liu et al*., 2013; *Lauzier et al*., 2013]. This knowledge is essential for the design of protocols and error correcting codes optimized for BAN applications. Due to the often repetitive nature of human body movement caused by both physiological and biomechanical processes, it is anticipated and indeed expected that noticeable correlation may exist between current and previous observations of the received signal [*Cotton et al*., 2009d]. A function that is useful for determining the variation of a stochastic process is the autocorrelation function (ACF). At present, our understanding of the autocorrelation in body area networks is somewhat limited. In *Smith et al*. [2009a] a Weibull correlation function was fitted to the amplitude data for a number of on-body channels assuming isotropic signal reception. The authors averaged a number of distinct on-body channels for walking and running scenarios and showed that the Weibull ACF best described the temporal data. In *Cotton et al*. [2009d] autoregressive models were constructed after considering the autocorrelation statistics of the fading amplitude in BANs. Here the autocorrelation and cross-correlation functions were shown to be dependent on body state and surroundings. The multilink cross-correlation function is also investigated in *van Roy et al*. [2013] together with the autocorrelation. The strong (repetitive) cross-correlation pattern between many of the links was found to be due to the temporal movement of the limbs.

In both *Cotton et al*. [2013] and *Liu et al*. [2013], the Doppler characteristics of on-body channels have been investigated at 2.45 GHz and also at 4.2 GHz in *Liu et al*. [2013]. Using a complex received signal model which considers a nonisotropic scattered signal contribution along with the presence of an optional dominant signal component, the authors of *Cotton et al*. [2013] used an ACF derived for mobile-to-mobile communications to model the temporal behavior of a range of dynamic body area network channels with considerable success. It was also shown that the complex mobile-to-mobile ACF provides an improved fit to on-body channel data for the left-waist to right-ankle channel when compared to Clarke's model. The Doppler spectra of on-body channels in tangential and normal polarization to the body were measured, then modeled (using the three-cylinder model of *Liu et al*. [2011]) and compared statistically in *Liu et al*. [2013]. By analyzing two aspects of body dynamics, namely, periodic dynamic body scattering by repetitive motion and the mobility of nodes also caused by body movements; it was found that the local and periodic body scattering caused Doppler spreads and significant frequency harmonics on the Doppler spectra. The authors proposed an experimental model to describe the overall and/or local Doppler spectra for periodic channels in anechoic environments:

$$\mathrm{PSD}(f_D) = \frac{1}{1 + wf_D^2} + \sum_{m \neq 0}^{\infty} \frac{1}{mz + w(f_D - mf_0)^2} \frac{1}{xy^{(m-1)}} \tag{9}$$

where $f_D$ is the Doppler frequency, $w$ is the spread parameter inversely proportional to the Doppler spread, $f_0$ is the fundamental frequency, $m$ is the order of the harmonics, $x$ and $y$ describe the global and local decaying of the power spectrum density (PSD) at the frequency harmonics, and $z$ describes the local Doppler spread at harmonics.

Other second-order statistics such as the level crossing rate (LCR) and average fade duration (AFD) which can be used to estimate the rate of occurrence and duration of fades, respectively, have been used to model the temporal behavior of signal variation in on-body channels [*Cotton and Scanlon*, 2007a, 2009a; *Hu et al*., 2007; *Chaganti et al*., 2010]. In *Cotton and Scanlon* [2007a] and *Chaganti et al*. [2010] lognormal higher-order statistics are shown to provide a good fit to measured channel data. In particular, Chaganti *et al*. [*Chaganti et al*., 2010] measured 40 simultaneous links over a few hours of everyday activity at 2.4 GHz. They considered two test subjects, namely an adult male and an adult female and found that the channel data for the female showed a better fit to the lognormal second-order statistics. Theoretical equations for the LCR and AFD in


©2014. The Authors.

Nakagami-*m* and Rice fading channels were also considered for the on-body links analyzed in *Cotton et al*. [2009b]. Here simultaneous measurements of the fading observed in on-body channels covering the head, chest, waist, and ankle areas of the body were conducted in three separate environments—an anechoic chamber, an open office area, and a hallway at 2.45 GHz. Although each model was selected using the Akaike Information Criterion [*Akaike*, 1974] for particular links, overall the Nakagami-*m* fading model was selected most often to model the second-order statistics of the channels considered.

## 3. Ultrawideband Channel Models

Ultrawideband (UWB) technology is defined by a signal bandwidth exceeding 500 MHz or 20% of the operating frequency. The large available bandwidth enables the use of a low power spectral density and provides a number of advantages such as a low interference probability, a limited sensitivity to fading, a positioning capability, and a reduced complexity of system design. Hence, UWB has quickly been considered as a key technology for BANs, resulting in a large number of channel characterizations and modeling studies [*Kobayashi*, 2009], also including the IEEE 802.15.4a [*IEEE*, 2007] and 802.15.6 [*IEEE*, 2012] standardization efforts.

### 3.1. UWB Channel Measurements

Analogous to narrowband measurements, UWB channel measurements usually rely on a vector network analyzer spanning the 3–10 GHz frequency range, with some authors restricting the range to 3–6 GHz or 6–10 GHz. Scenarios again cover anechoic and indoor environments, with both LOS and NLOS transmissions. Some studies also restrict the Tx and Rx node locations to specific body areas, such as the chest and waist. Measured parameters include the path loss and the UWB channel impulse response (CIR), whose properties are then fitted by stochastic distributions. In *van Roy et al*. [2010], multiantenna UWB channels are further measured, in order to characterize the cross-correlation properties of the CIR among different antennas. The parameters used to characterize continuous power delay profiles or discrete tap delay lines include the received power of the first tap (or the equivalent path loss), the power decay, the fading statistics of each tap, and possibly the intertap correlation. In the following, we briefly describe the main results for each of these parameters.

### 3.2. Path Loss Models

As already pointed out, the large variety of BAN links makes it quite challenging to fit a single distance-dependent model to all scenarios. Hence, a large number of path loss models simply consist in a quantitative loss (or received power) for each type of link, or to statistically describe all possible values by a probability density function with a mean value and a standard deviation [*Di Bari et al*., 2013]. Alternatively, a few distance-dependent path loss models have been derived in specific scenarios, analogous to Section III-A. In particular, *Fort et al*. [2006] recommended the use of a power decay law for links around the torso, so that the path loss reads as

$$P_{\mathrm{dB}}(d) = P_0 + 10n\log_{10}\left(\frac{d}{d_0}\right) + N \tag{10}$$

where $n = 7.2$ is the path loss exponent and $N$ is a normally distributed variable with zero mean and standard deviation $\sigma_N$. For links alongside the body, *Zasowski et al*. [2003] has derived values of $n$ equal to 3.3 in anechoic conditions and 2.7 indoors. By contrast, *van Roy et al*. [2010] has fitted the distance dependence around the torso with an exponential model,

$$P_{\mathrm{dB}}(d) = P_0 + m(d - d_0) + N \tag{11}$$

with $m = 1.26$ dB/cm. Finally, it must be noted that only a slight increase of the path loss with frequency has been found [*Fort et al*., 2006].

Building upon the results in *Fort et al*. [2006], the IEEE 802.15.4a standard has proposed UWB channel models [*Molisch et al*., 2006] for different applications including on-body communications, all using (10) as path loss model. In its initial version, the model was extracted from electromagnetic simulations over a 2-6 GHz frequency range, and restricted to scenarios with antennas located only on the torso, in anechoic chamber environments with ground echoes, which may be considered as a representation of an open space environment. The electromagnetic simulations emphasized the existence of creeping waves around the torso and the quasi nonpenetration of the waves in the body for frequencies in the GHz range. Therefore, the distance between the transmitter and the receiver was defined around the perimeter of the body instead of a straight line through the body.


©2014. The Authors.

**Table 5.** CM3A Model for UWB

| Parameter | Hospital Room | Anechoic Chamber |
|---|---|---|
| $d_0$ (mm) | 1 | 1 |
| $n$ | 1.92 | 3.41 |
| $P_0$ (dB) | 3.38 | -31.40 |
| $\sigma_N$ (dB) | 4.40 | 4.85 |

Further measurement campaigns in the 3.1–10.6 GHz frequency band have been carried out for UWB on-body channel modeling in the framework of IEEE 802.15.6 [*IEEE*, 2012] to better estimate the parameters of (10), whose values are summarized in Table 5.

Note that another path loss model (CM3B) is proposed in the standard, based on another measurement campaign described in *Dolmans and Fort* [2008] and based on the results of *Fort et al.* [2006]. Recently, *Kumpuniemi et al.* [2013] estimated path loss exponents from 2.6 to 3.3, respectively, for loop and dipole antennas, together with values of $\sigma_N$ ranging from 12 to 14 dB, in anechoic conditions. It was also noted that the propagation delay in the antenna structures, if not compensated, may lead to large errors in the parameter estimation.

### 3.3. Empirical Tap Delay Line Models

As mentioned earlier, the vast majority of empirical models are based on the stochastic characterization of the UWB CIR, using measurements to define continuous power delay profiles or discrete tap delay line models. A tap delay line model defines the CIR as a set of $L$ complex paths, each being characterized by its amplitude $a_l$, phase $\phi_l$, and delay-of-arrival $\tau_l$ (usually normalized to the first path):

$$h(t,\tau) = \sum_{l=1}^{L} a_l(t)\exp(j\phi_l)\delta(\tau-\tau_l) \tag{12}$$

In some cases, the paths are grouped into clusters, so that the general model reads as

$$h(t,\tau) = \sum_{m=1}^{M}\sum_{l=1}^{L_m} a_{ml}(t)\exp(j\phi_{ml})\delta(\tau-\tau_{ml}) \tag{13}$$

where $M$ is the number of clusters (usually $M=1$ or 2), and $L_m$ is the number of paths in the $m$th cluster.

The first characteristic of any tap delay line model is the modeling of the amplitude. It is usually considered as a fading variable, whose mean is decreasing as a function of its respective delay. In most studies, a single cluster is considered ($M=1$), and the amplitude decay is modeled by a single slope:

$$\begin{aligned} a_l|_{\mathrm{dB}} &= 10\cdot\log_{10}\left[\exp\left(-\frac{\tau_l}{\Gamma}\right)\right] - P_{\mathrm{dB}} + S \\ &= -4.34\frac{\tau_l}{\Gamma} - P_{\mathrm{dB}} + S \end{aligned} \tag{14}$$

where $P_{\mathrm{dB}}$ is given by the path loss model, $\Gamma$ is the decay rate of the multipath profile, and $S$ is a stochastic term representing the additional fading behavior of each tap, usually considered as lognormal (i.e., modeled by a Gaussian variable in dB scale), as discussed later.

Values of the decay rate have been empirically derived in numerous studies and are summarized in Table 6 for single-cluster models.

Regarding the number of resolvable paths (or taps) given by $L$ in (12), it is usually taken as a Poisson variable, whose mean value naturally depends on the selected threshold. For a 20 dB threshold below the largest path, the mean number of paths in indoor environments is found to be within the range of 41 to 66 in *Di Bari et al.* [2013], in line with the value of 38 prescribed by IEEE 802.15.6 standard. Surprisingly, values in Table 6 vary

**Table 6.** UWB Tap Delay Line Model Parameters

| | Anechoic | | | | Indoor | | | |
|---|---|---|---|---|---|---|---|---|
| | *Aoyagi et al.* [2008] | *Chen et al.* [2011] | *Di Bari et al.* [2013] | *Fort et al.* [2006] | *Aoyagi et al.* [2008] | *Yazdandoost and Sayrafian-Pour* [2010] | *D'Errico and Ouvry* [2010b] | *Di Bari et al.* [2013] |
| $\Gamma$ (ns) | 8.9 | 29.8 | 13.4 (LOS)<br>11.9 (NLOS)<br>14.2 (generic) | 0.3 (LOS)<br>0.46 (NLOS) | 155.7 | 59.7 (NLOS) | 22.3–29.0 | 16.5 (LOS)<br>49.3 (NLOS)<br>24.6 (generic) |
| $\sigma_S$ (dB) | 2.9 | 4.6 | 11.7 | 5.4 (LOS)<br>4.6 (NLOS) | 4.9 | 5.0 | 4.02–4.62 | 10.0 |


©2014. The Authors.

significantly from one dataset to another, especially in the anechoic case as far as $\Gamma$ is concerned. While some reference papers do not provide many details regarding the corresponding experimental setup, we could gather the following arguments.

1. On the one hand, values in *Chen et al*. [2011] are extremely large, while power delay profiles look quite unrealistic: these values should in our opinion be taken with great caution.
2. On the other hand, values in *Fort et al*. [2006] are much smaller: this can be explained by the fact that these values were extracted on the body wave only, removing all other paths by time gating. Hence, they actually correspond to a single path with very little dispersion.
3. Finally, values in *Aoyagi et al*. [2008] and *Di Bari et al*. [2013] are intermediate, but it must be noted that the measurements included reflections off the arms and legs (given), rather than only the surface wave around the torso [*Fort et al*., 2006] and were taken in semianechoic conditions, which means that the power delay profile includes the ground reflection, which explains the larger decay rates.

The model described above, as outlined by (14), is single-cluster model. A two-cluster model is used in *Fort et al*. [2006] and *Viittala et al*. [2009] to represent indoor scenarios, the first cluster corresponds to on-body propagation, whereas the second cluster is caused by interactions with the surrounding environment or by the ground reflection. In this case, each cluster is characterized by an equation similar to (14), with a specific value of the decay rate for each cluster, i.e., $\Gamma_1$ for the first cluster and $\Gamma_2$ for the second cluster. In particular, the model developed by *Fort et al*. [2006], which corresponds to propagation around the torso, recommends values of $\Gamma_1$ ranging from 300 $\mu$s (front/LOS) to 460 $\mu$s (back/NLOS), as well as similar values for $\Gamma_2$ (the ground reflection is, however, attenuated by ~40 dB with respect to the first cluster, so it is questionable whether it must be included in practice). Note that *Fort et al*. [2006] also considers that taps at different delays are correlated within the first cluster (corresponding to the on-body wave) with a correlation coefficient as high a 0.8.

In *van Roy et al*. [2010], a dual-slope (or two-cluster) model is also identified for anechoic conditions, considering propagation links around the body torso. Intuitively, each cluster corresponds to one propagation direction around the body, and the breakpoint delay corresponds to the relative delay of the second cluster (i.e., waves arriving from the opposite direction with respect to the first cluster). Measurements have shown that the first slope becomes slightly sharper for increasing distances between the *Tx* and *Rx*, with an average value of $\Gamma_1 = 240$ $\mu$s, which is close to the values of *Fort et al*. [2006]. By contrast, the second slope (still corresponding to on-body propagation) is a constant, $\Gamma_2 = 1$ ns. Finally, the extension proposed in *D'Errico and Ouvry* [2010b] deals with dynamic scenarios starting from real-time UWB measurements. The parameterization is also given in Table 6.

In the model above, the fading of each tap is modeled by the variable *S*. Some authors make a distinction between large-scale and small fading, and suggest that both types of fading are lognormal. Alternatively, some models only consider one lognormal fading, without specifying its scale. Indeed, because of the ultrawide bandwidth, small-scale fading is usually limited, and in any case hardly Rayleigh distributed. This unfortunately implies that it cannot be easily separated from large-scale fading. For this reason, most studies fit the global variations of *S*, considered as the combination of small- and large-scale fading, by a lognormal distribution, i.e., *S* is Gaussian distributed with a standard deviation $\sigma_S$. The range of $\sigma_S$ strongly depends on the scenario and sometimes on the tap index. In anechoic conditions, values of $\sigma_S$ from roughly 3 to 10 dB are found in the literature, as outlined in Table 6. One important mechanism, explaining for the higher values, is the ground reflection, which was not avoided in *Di Bari et al*. [2013], even in anechoic conditions. A large number of measurements have restricted the analysis to propagation around the torso. In this case, the standard deviation as measured in *van Roy et al*. [2010] and *Molisch et al*. [2006] varies for anechoic environments from ~3.9 dB (front/LOS propagation, first tap) to ~6 dB for all others taps (including side and front-to-back NLOS propagation). In semianechoic conditions (i.e., when ground reflection is taken into account), $\sigma_S$ reaches up to 11.7 dB [*Di Bari et al*., 2013].

### 3.4. Physical UWB Channel Models

A number of numerical and physical approaches have also been investigated in the context of UWB BAN. In particular, *Tiberi et al*. [2012] has extended the work of *Fort et al*. [2010] to consider UWB and more complex body models: the body is described as multilayered stratified cylinders, whose electromagnetic parameters are taken as frequency varying. This is carried out by extrapolation of the electromagnetic properties of tissues over the whole UWB spectrum based on the Debye model [*Li and Hagness*, 2001; *Gabriel et al*., 1996;


©2014. The Authors.

*Mrozowski and Stuchly*, 1997; *Wuren et al*., 2007]. Simulations were carried out in the frequency domain, by deriving the narrowband solution at a number of frequency components and by filtering the transmitting signal spectrum with the so-obtained frequency transfer function.

## 4. Off-Body and Body-to-Body Channel Models

Although a lot of effort has been generated toward the study of propagation dynamics and channel characteristics for on-body communications, *body-to-body* (or *interbody*) as well as *off-body* channels have received relatively little attention. In this section we provide a general overview of the current research on channel modeling for these emerging body centric networking applications.

### 4.1. Body-to-Body Communications

A number of research teams have performed measurement campaigns with the aim of characterizing the interbody channel. In particular Cotton et al. [*Cotton and Scanlon*, 2008; *Cotton*, 2009e] have provided a statistical description of dynamic body-to-body channels at 2.45 GHz. They considered a scenario representative of indoor sweep and search operations for fire and rescue personnel, where four subjects moved within a building. One of the firefighters was fitted with a transmitter while the other three played the role of the receivers. The authors demonstrated that the $\kappa$-$\mu$ distribution was able to provide a good fit to the distribution of small-scale fading for all the considered links, in comparison to other fading models such as Nakagami-*m*, lognormal, Rice, and Weibull. The observation of low cross correlation and comparable mean signal levels in these studies led the authors to suggest the idea of employing spatial diversity to improve channel performance in body-to-body communications. Similar conclusions on diversity were also presented in *Wang* [2009] and [*Pedersen et al*., 2009]. Here wideband channel measurements were conducted at a carrier frequency of 5.5 GHz in an indoor environment. Considering the classical distance-dependent path loss model, the authors proposed an inter-BAN channel model where the shadowing is best described by a lognormal distribution and the path loss exponent results were always found to be smaller than 2.

Another statistical description of the inter-BAN channel is given in *Hu et al*. [2010a] and *Hu et al*. [2010b]. The authors investigated propagation characteristics in frequency bands centered at 2.45 GHz and 5.8 GHz through an extensive measurement campaign involving two subjects (one with the transmit antenna and the other equipped with the receiving devices) in an office environment. The users were positioned considering different distances between each other while performing various random activities with random body orientations. Variations of the channel path gain were found to follow a gamma distribution with mean and variance values following a power law in respect to the distance between the two BANs. The rate of decrease was found to be almost independent of the considered frequency, while strictly related to the on-body position of the device, and body orientation. Moreover, the short-term fading turned out to be described by a Rice distribution with the *K*-parameter depending more on the on-body position of the antenna than the separation distance, while the long-term fading followed either a gamma distribution (when the distance between the subjects remained constant) or a lognormal one (if the distance also changed randomly). For this distribution, the mean and the variance decrease with the distance followed a power law, with the rate of decrease almost independent from the frequency band but strictly related to the antenna position.

Investigations on UWB interbody communications have been performed in *See et al*. [2009]. Measured data obtained in an anechoic chamber environment for two subjects standing at various distances with different body orientations showed that the path loss, calculated through the classical distance-dependent formula, was strongly related to the placement of the devices on the body as well as to the relative position of the human bodies. In *Hanlen et al*. [2009] and *Zhang et al*. [2009], the authors performed some measurements focusing on coexistence problems when multiple BANs are colocated. Since none of the networks has the governance to control the transmission of other colocated BANs, this provides the potential for interference which could lead to a severe degradation of BAN performance. By collecting the received signal strength indicator values of all the investigated links (reference and interferer), the authors found that the interference signal power is dominated by factors which are not related to the distance but mostly subject movements, both local (e.g., arm swinging) and global (i.e., walking or running). Moreover, the results showed that the Signal-to-Interference Ratio could be low or even negative, since the interferers were often more powerful than the reference link because of the significant shadowing effect of the human body that could lead to a power absorption of up to 60 dB. Furthermore, the authors also investigated whether the reference and the


©2014. The Authors.

interferer links were sufficiently independent, such that, it would be possible to measure them separately and later combine them. The computation of correlation coefficients revealed that the two signals were generally uncorrelated and also statistically independent when considered over large periods of time (on the order hundreds of seconds). Conversely, considering short intervals, it was found that two channels may show correlation, in particular when subject movement is not the main source of channel dynamics (and hence it varies slowly). In *De Silva et al*. [2009], the authors propose a solution to mitigate the interference problem using a fixed network infrastructure to monitor those BANs that are more likely to interfere with each other. Another solution is also proposed in *Khan et al*. [2010] where diversity brought by Multiple Input Multiple Output (MIMO) technique is exploited not only for interference rejection but also for increasing channel capacity.

Ray tracing methods have also been used recently in *Kouitas* [2009] for off-body and body-to-body communications. The 2-D scenario considered in this work does not take into account the environment around the bodies and the latter are modeled as closed cylindrical surfaces with constitutive parameters chosen based on the "muscle" model. This approach could represent a powerful building block in the perspective of modeling inter-BAN communications (i.e., at least the part which does not involve an interaction with the environment). In *Cotton* [2009f] and *Cotton et al*. [2010a], the authors present an approach to simulate dynamic soldier-to-soldier signal propagation using a combination of animation-based technology, which takes into account real body movements (using the Poser7 software tool), a computer generated environmental model (using the AutoCAD software package from Autodesk), and a commercial ray-launching engine to perform channel prediction. The reference scenario, in this case, was that of millimeter-wave (60 GHz) soldier-to-soldier communications for counter-insurgency cordon and sweep operations. The authors simulated the field of action and the realistic movement of a team of four soldiers to extract important channel metrics such as the root-mean-square angle of arrival and delay spread. They found that for an outdoor 60 GHz soldier-to-soldier (body-to-body) link the vast majority of the energy is contained within the direct path, which typically arrives within 25 ns. The authors also noted the existence of occasionally significant multipath components that arrive between 100 and 150 ns. For the same scenario, the azimuth RMS angle spread had a 90% probability of being less than 90°. The corresponding figure for the elevation RMS angle spread was lower at 20°. These results demonstrate the directional characteristics of the outdoor 60 GHz soldier-to-soldier transmission channel and the potential for beamforming arrays to provide a good degree of covertness for this type of body centric application.

In *Cotton et al*. [2010b], the same team of researchers realized a simulated study of the cochannel inter-BAN interference at 2.45 GHz and 60 GHz. Using an accurate computer-aided design (CAD) model of an indoor location together with a human body model obtained through the use of the Poser7 animation software and a full 3-D ray-launching simulator tool, the authors found that on-body communications at 2.45 GHz were heavily susceptible to interference caused by undesired signal reception from other nearby BANs, while operating BANs at the 60 GHz frequency generally provided a mitigation of cochannel interference, allowing a greater number of networks to coexist.

### 4.2. Off-Body Channels

One of the earliest attempts at providing a complete insight into the characteristics of the off-body channel has been presented in *Ziri-Castro et al*. [2004]. The authors performed a comparison between measured data and simulations of a narrowband 5.2 GHz radio channel for two indoor environments (a corridor and an office). The measurements involved one fixed transmitter and one receiver placed on the hip of a subject walking toward (LOS conditions) and away (NLOS conditions) from the transmitting antenna, whereas the simulations were performed using a three-dimensional image-based propagation prediction technique. The use of a simulation tool seemed to be appropriate for the LOS case but revealed some inaccuracies in NLOS situations. A statistical analysis of the small-scale fading found that a combination of the Rayleigh (signal level below the mean) and lognormal (signal level above the mean) distributions provided the best fit for the corridor environment, whereas in the office case the lognormal distribution provided the optimum fit.

Off-body communications at 868 MHz were studied in *Cotton and Scanlon* [2007b]. Here measurements were conducted by considering several receiving antennas placed on the subject's body, different environments (i.e., anechoic chamber, open office, and hallway), LOS and NLOS conditions and a walking movement. An analysis of the channel data found that both antenna positioning and human body movement play an extremely important role in indoor propagation characteristics for wearable systems. Moreover, it has been


©2014. The Authors.

verified that the Nakagami-*m* distribution provided the optimum fit for the majority of the off-body propagation channels investigated in both anechoic and indoor multipath environments. This distribution turned out to be suitable for the considered scenarios as, differently from other distribution like Rice or Rayleigh, it does not assume scattered components of equal amplitude. The LCR and AFD were also considered and were found to be well described by Nakagami second-order statistics.

In *Cotton and Scanlon* [2007c] the cross-correlation level between the fading experienced at different body locations was also evaluated, the low values found suggested the idea that a spatial diversity combining scheme could improve significantly the system performances. A similar experiment was also presented in *Smith et al.* [2009b], where the authors performed a measurement campaign which collected real-time channel responses at the carrier frequencies of 820 MHz and 2.36 GHz for a subject equipped with two antennas either standing still in front of a fixed receive antenna, changing body orientation and the relative distance, or performing a walk toward the receiving device. Different statistics were compared in order to find the one that best describes the received signal amplitude. Overall, it was found that the lognormal distribution provided the most reliable fit for both the considered bands. In order to evaluate the channel stability, the authors introduced a new parameter called channel variation factor and calculated the ratio between the standard deviation and the root-mean-square power of a channel response sequence. The off-body channel turned out to be quite stable, more so at 820 MHz than at 2.36 GHz, with a coherence time in the order of tens of milliseconds. In this study it was also found that the on-body device position also played a significant role in the channel temporal stability.

Considering the great advantages that the use of UWB could bring to the system performances in terms of reduction of multipath fading, the possibility of reaching high data rates and a reduction in operating power, some researchers have also focused on the characterization of the channel at UWB frequencies. In [*Goulianos et al.*, 2008a, 2008b, 2008c] the authors proposed to model the off-body communication channel with a multislope path loss equation obtained from the study of propagation mechanisms around the body (creeping waves) combined with the traditional distance-dependent path loss formula. Based on the measured data, statistical channel parameters have been extracted with respect to both the radial coordinate $\rho$, denoting the distance between the transmitter and the body center, and the body orientation angle $\Theta_A$, which is formed by the lines connecting the body center to the transmitter and to the on-body antenna, respectively. Mathematically the model is expressed as

$$L(\rho,\theta_A)=\begin{cases} L_0(\rho)-n_\theta(\theta_A)(\theta_A-\theta_0), & 0\le\theta_A\le\theta_{AL}(\rho) \\ L(\theta_{AL})-n_\theta(\theta_A)[\theta_A-\theta_{AL}(\rho)] & \theta_{AL}(\rho)\le\theta_A\le\theta_{AS}(\rho) \\ L(\theta_{AS})-n_\theta(\theta_A)\left[\theta_A-\theta_{AS}(\rho)^{\mathrm{AS}}\right] & \theta_{AS}(\rho)\le\theta_A\le\pi \end{cases} \tag{15}$$

where $L_0(\rho)$ is represented by

$$L_0(\rho)=L_0(\rho_0)+10n_\rho\log_{10}\left(\frac{\rho}{\rho_0}\right) \tag{16}$$

and $\theta_{AL}$ and $\theta_{AS}$ are the breaking point angles, which are defined as the angle after which the decay coefficient $n_\theta(\theta_A)$ changes its arithmetic value. These angles indicate, respectively, the passage from the lit zone and from the shadow region of the transmitter. Power delay profile analysis and modeling were also performed.

Focusing on a real hospital environment in *Catherwood and Scanlon* [2009], the authors presented a measurement campaign for stationary and mobile UWB off-body channels. In mobile scenarios both LOS and NLOS cases tended to have lognormally distributed fading with the latter having significantly lower mean signal strength. In stationary conditions, the signal strength results were also dependent on user orientation. An off-body channel model was also proposed for UWB in IEEE 802.15.6 [*Sawada et al.*, 2008], resulting in a channel model which was very close to the free-space indoor UWB one, such as the one proposed in IEEE 802.15.4a [*Molisch et al.*, 2006]. In *Taparugssanagorn et al.* [2010a, 2010b], the authors investigated the UWB channel for both on-body and off-body communications. Different movements in hospital environments have been addressed and a two-state Weibull renewal process was proposed to describe the channel dynamics with a low-complexity model.

## 5. Advanced Topics in BAN Channel Modeling

The previous sections have shown that the literature on BAN channel modeling is wide and extensive. Nevertheless, a large dispersion of the results and models can be observed, in particular with respect to the


©2014. The Authors.

path loss and fading statistics. This is partially due to the fact that each measurement has been carried out with different methodologies but also the intrinsic characteristics of BANs. Indeed it has to be mentioned that when talking about channel modeling for BANs, we should consider that antennas are included in the radio channel. Some general features of the antenna effect have been pointed out in *Hall et al*. [2007], showing that antennas with polarization normal to the body surface are generally advantageous for on-body propagation. This is due to the fact that on-body propagation mainly occurs by creeping wave and surface wave, which are opportunely excited by the normal polarization. This has also recently pointed out in *Rosini and D'Errico* [2012b], showing that the polarization affects not only the path loss but also the slow fading and multipath fading characteristics. For instance, the use of normal polarization decreases the shadowing and increases the Rice *K* factor of the small-scale fading distribution, confirming the idea that a dominant signal path exists. The effect of the antenna has also been analyzed in *Rosini et al*. [2012] and *Rosini and D'Errico* [2012a] for off-body and body-to-body communications.

The creation of universal body centric channel models could be greatly enhanced by antenna de-embedding. On the one hand this would be difficult to achieve for on-body channels, since it is hard to estimate the paths' angles of arrival since antennas cannot be considered in the far field. On the other hand the antenna can be affected differently by the body according to its position, and the body characteristics itself which change from person to person. Hence, even if the antenna de-embedding could be achieved in principle for off-body and body-to-body communications, an antenna model is required to take into account the variability. To this end, a statistical approach for antenna modeling has been presented in *Mackowiak et al*. [2012] and eventually combined with dynamic phantoms [*Mackowiak and Correia*, 2011]. Moreover, spherical wave expansion has been utilized to understand the antenna behavior on the body and de-embed it from the radio channel [*Aoyagi et al*., 2013].

Additionally, body dynamics and their impact on space-time correlation also need further investigation, especially for body-to-body and off-body channel [*Rosini and D'Errico*, 2013]. Generally, the correlation analysis is carried out on star-topologies networks, while cooperative approaches will require a full-mesh description. First, results in this area for the on-body channel at 4.2 GHz have been presented in *van Roy et al*. [2013]. Further work must also be conducted to extend the work to other frequency bands. In this context, a common framework of channel modeling is a prerequisite to compare results from different research teams, going beyond the channel models currently presented in literature and by standardization bodies.

Within the remit of the COST IC1004 Action [*IC1004*, 2014], the Topical Working Group on Body Area Networks, has brought together a number of different worldwide institutes who are working to overcome the difficulties of channel modeling in BANs with the aim of producing a unique reference for the scientific community. First attempts have been made before in *Liu et al*. [2011], and more recently in *Mackowiak et al*. [2013]. The outcomes of this Working Group are expected in 2015.

## 6. Summary

This paper provides a survey of recent results in radio propagation and channel modeling for wireless body area networks. We have addressed both narrowband and UWB on-body channels, together with off-body and body-to-body scenarios. In each case, we have reviewed popular examples that are widely used for the design and evaluation of BANs, highlighting and commenting on the main differences between results. Furthermore, the most important features of modeling efforts proposed in the context of recent wireless standards and collaborative actions were summarized. Finally, we have discussed some open problems relating to channel features not sufficiently reproduced by current channel models.

**Acknowledgments**
This work was supported by the U.K. Royal Academy of Engineering and the Engineering and Physical Research Council (EPSRC) under Grant Reference EP/H044191/1 and by the Leverhulme Trust, UK through a Philip Leverhulme Prize.

## References

Akaike, H. (1974), A new look at the statistical model identification, *IEEE Trans. Autom. Control*, *19*, 716–723.
Alomainy, A., Y. Hao, A. Owadally, C. G. Parini, Y. Nechayev, C. C. Constantinou, and P. S. Hall (2007), Statistical analysis and performance evaluation for on-body radio propagation with microstrip patch antennas, *IEEE Trans. Antennas Propag.*, *55*(1), 245–248.
Aoyagi, T., J. Takada, K. Takizawa, H. Sawada, N. Katayama, K. Y. Yazdandoost, T. Kobayashi, H.-B. Li, and R. Kohno (2008), IEEE 802.15-08-0416-04-0006: Channel Models for wearable and implantable WBANs – NICT, IEEE 802.15 Task Group 6 Document.
Aoyagi, T., M. Kim, and J. Takada (2013), Characterization for a electrically small antenna in proximity to human body—Towards antenna de-embedding in body area network channel modeling, 7th European Conference on Antennas and Propagation, 3421-3422, Apr. 2013.
Boulis, A., D. Smith, D. Miniutti, L. Libman, and Y. Tselishchev (2012), Challenges in body area networks for healthcare: The MAC, *IEEE Commun. Mag.*, *50*(5), 100–106.


©2014. The Authors.

Catherwood, P. A., and W. G. Scanlon (2009), Link characteristics for an off-body UWB transmitter in a hospital environment, loughborough antennas & propagation conference, November 2009.
Chaganti, V., D. B. Smith, and L. W. Hanlen (2010), Second-order statistics for many-link body area networks, *IEEE Antennas Wirel. Propag. Lett.*, *9*, 322–325.
Chahat, N., G. Valerio, M. Zhadobov, and R. Sauleau (2013), On-body propagation at 60 GHz, *IEEE Trans. Antennas Propag.*, *61*(4), 1876–1888.
Chandra, R., and A. J. Johansson (2013), An analytical link-loss model for on-body propagation around the body based on elliptical approximation of the torso with arms' influence included, *IEEE Antennas Wirel. Propag. Lett.*, *12*, 528–531.
Chen, Y., J. C. Y. Teo, J. Lai, E. Gunawan, K.-S. Low, C.-B. Soh, and P. B. Rapajic (2009), Cooperative communications in ultra-wideband wireless body area networks: Channel modeling and system diversity analysis, *IEEE J. Sel. Areas Commun.*, *27*(1), 5–16.
Chen, X., X. Lu, D. Jin, L. Su, and L. Zeng (2011), Channel modeling of UWB-based wireless body area networks, IEEE International Conference on Communications (ICC).
Conway, G. A., and W. G. Scanlon (2009), Antennas for over-body-surface communication at 2.45 GHz, *IEEE Trans. Antennas Propag.*, Special Issue on Antennas and Propagation on Body-Centric Wireless Communications, *57*(4), 844–855.
Conway, G. A., W. G. Scanlon, C. Orlenius, and C. Walker (2008), In situ measurement of UHF wearable antenna radiation efficiency using a reverberation chamber, *IEEE Antennas Wirel. Propag. Lett.*, *7*, 271–274.
Conway, G. A., W. G. Scanlon, S. L. Cotton, and M. J. Bentum (2010), An analytical path-loss model for on-body radio propagation, URSI International Symposium on Electromagnetic Theory (EMTS), 332–335, 16-19 Aug. 2010.
Cotton, S. L., and W. G. Scanlon (2006), A statistical analysis of indoor multipath fading for a narrowband wireless body area network, IEEE 17th International Symposium on Personal, Indoor and Mobile Radio Communications, 11-14 Sept. 2006.
Cotton, S. L., and W. G. Scanlon (2007a), Higher order statistics for lognormal small-scale fading in mobile radio channels, *IEEE Antennas Wirel. Propag. Lett.*, *6*, 540–543.
Cotton, S. L., and W. G. Scanlon (2007b), Characterisation and modeling of the indoor radio channel at 868MHz for mobile bodyworn wireless personal area network, *IEEE Antennas Wirel. Propag. Lett.*, *6*, 51–55.
Cotton, S. L., and W. G. Scanlon (2007c), Spatial diversity and correlation for off-body communications in indoor environments at 868MHz, IEEE Vehicular Technology Conference, April 2007.
Cotton, S. L., and W. G. Scanlon (2008), The $k$-$\mu$ distribution applied to the analysis of fading in body to body communication channels for fire and rescue personnel, *IEEE Antennas Wirel. Propag. Lett.*, *7*, 66–69.
Cotton, S. L., and W. G. Scanlon (2009a), An experimental investigation into the influence of user state and environment on fading characteristics in wireless body area networks at 2.45 GHz, *IEEE Trans. Wireless Commun.*, *8*(1), 6–12.
Cotton, S. L., G. A. Conway, and W. G. Scanlon (2009b), A time-domain approach to the analysis and modeling of on-body propagation characteristics using synchronized measurements at 2.45 GHz, *IEEE Trans. Antennas Propag.*, *57*(4), 943–955.
Cotton, S. L., and W. G. Scanlon (2009c), Characterization of the on-body channel in an outdoor environment at 2.45 GHz, 3rd European Conference on Antennas and Propagation (EuCAP), 722–725, 23–27 March 2009.
Cotton, S. L., W. G. Scanlon, and G. A. Conway (2009d), Autocorrelation of signal fading in wireless body area networks, IET Seminar on Antennas and Propagation for Body-Centric Wireless Communications, 20-20 April 2009.
Cotton, S. L., and W. G. Scanlon (2009e), Channel characterization for single- and multiple-antenna wearable systems used for indoor body-to-body communications, *IEEE Trans. Antennas Propag.*, *57*(4), 980–990.
Cotton, S. L., W. G. Scanlon, and B. K. Madahar (2009f), Millimeter-wave soldier-to-soldier communications for covert battlefield operations, *IEEE Commun. Mag.*, *47*(10), 72–81.
Cotton, S. L., W. G. Scanlon, and K. B. Madahar (2010a), Simulation of millimetre-wave channels for short-range body to body communications, 2010 Proceedings of the Fourth European Conference on Antennas and Propagation (EuCAP), 12–16 April 2010.
Cotton, S. L., W. G. Scanlon, and P. S. Hall (2010b), A simulated study of co-channel inter-BAN interference at 2.45 GHz and 60 GHz, 2010 European Wireless Technology Conference (EuWIT), 61–64, 27–28 Sept. 2010.
Cotton, S. L., A. McKernan, A. J. Ali, and W. G. Scanlon (2011), An experimental study on the impact of human body shadowing in off-body communications channels at 2.45 GHz, 5th European Conf. Antennas and Propagation (EUCAP), 3133–3137, Rome, Italy, Apr. 2011.
Cotton, S. L., A. Meijerink, and W. G. Scanlon (2013), Characteristics of the complex received signal in dynamic body area networks, to be presented, International Symposium on Personal, Indoor and Mobile Radio Communications (PIMRC), London, Sept. 2013.
D'Errico, R., and L. Ouvry (2010a), A statistical model for on-body dynamic channels, *Int. J. Wireless Inform Network*, *17*, 92–104, September 2010.
D'Errico, R., and L. Ouvry (2010b), Delay dispersion of the on-body dynamic channel, European Conference on Antenna and Propagation (EuCAP 2010), 12–16 April 2010, Barcelona, Spain.
De Silva, B., A. Natarajan, and M. Motani (2009), Inter-user interference in body sensor networks: Preliminary investigation and an infrastructure based solution, Sixth International Workshop on Wearable and Implantable Body Sensor Networks.
D'Errico, R., and L. Ouvry (2009), Time-variant BAN channel characterization, IEEE 20th International Symposium on Personal, Indoor and Mobile Radio Communications, 3000–3004, 2009.
D'Errico, R., R. Rosini, and M. Maman (2011), A performance evaluation of cooperative schemes for on-body area networks based on measured time-variant channels, IEEE International Conference on Communications (ICC).
Di Bari, R., Q. H. Abbasi, A. Alomainy, and Y. Hao (2013), An advanced UWB channel model for body-centric wireless networks, *Prog. Electromagn. Res.*, *136*, 79–99.
Dolmans, G., and A. Fort (2008), IEEE P802.15-08-0418-01-0006, Channel Model WBAN—Holst Centre/IMEC-NL, IEEE 802.15 Task Group 6 Document, July 2008.
Filho, J. C. S. S., and M. D. Yacoub (2009), On the second-order statistics of Nakagami fading simulators, *IEEE Trans. Commun.*, *57*(12), 3543–3546.
Fort, A., C. Desset, P. de Doncker, P. Wambacq, and L. van Biesen (2006), An ultra-wideband body area propagation channel model—From statistics to implementation, *IEEE Trans. Microwave Theory Tech.*, *54*(4), 1820–1826.
Fort, A., C. Desset, P. Wambacq, and L. V. Biesen (2007), Indoor body-area channel model for narrowband communications, *IET Microwaves Antennas Propag.*, *1*(6), 1197–1203.
Fort, A., G. Roqueta, F. Keshmiri, C. Craeye, and C. Oestges (2010), A body area propagation model derived from fundamental principles: Analytical analysis and comparison with measurements, *IEEE Trans. Antennas Propag.*, *58*(2), 503–514.
Gabriel, C., S. Gabriely, and E. Corthout (1996), The dielectric properties of various tissues, *Phys. Med. Biol.*, *41*, 2231–2249.
Giddens, H., D.-L. Paul, G. S. Hilton, and J. P. McGeehan (2012), Influence of body proximity on the efficiency of a wearable textile patch antenna, 6th European Conference on Antennas and Propagation (EUCAP), 1353–1357.
Goulianos, A. A., T. W. C. Brown, and S. Stavrou (2008a), Ultra-wideband measurement and results for sparse Off-body communication channels, Loughborough Antennas and Propagation Conference, March 2008.


©2014. The Authors.

Goulianos, A. A., T. W. C. Brown, and S. Stavrou (2008b), A novel path-loss model for UWB off-body propagation, IEEE Vehicular Technology Conference, VTC Spring, May 2008.
Goulianos, A. A., T. W. C. Brown, and S. Stavrou (2008c), Power delay profile modeling of the ultra wideband off-body propagation channel, *IET Microwaves Antennas Propag.*, *4*(1), 62–71.
Hall, P., et al. (2007), Antennas and propagation for on-body communication systems, *IEEE Trans. Antennas Propag.*, *49*(3), 41–58.
Hanlen, L. W., D. Minutti, D. Rodda, and B. Gilbert (2009), Interference in body area networks: Distance does not dominate, 2009 IEEE 20th International Symposium on Personal, Indoor and Mobile Radio Communications, September 2009.
Hu, Z., Y. I. Nechayev, P. S. Hall, C. C. Constantinou, and Y. Hao (2007), Measurements and statistical analysis of on-body channel fading at 2.45 GHz, *IEEE Antennas Wirel. Propag. Lett.*, *6*, 612–615.
Hu, Z. H., Y. Nechyev, and P. Hall (2010a), Measurement and statistical analysis of the transmission channel between two wireless body area networks at 2.45 GHz and 5.8 GHz, ICECom 2010, September 2010.
Hu, Z. H., Y. Nechyev, and P. Hall (2010b), Fading of the transmission channel between two wireless body area networks in an office at 2.45 GHz and 5.8 GHz, Loughborough Antennas and Propagation Conference (LAPC), November 2010.
IC1004 (2014), Action on cooperative radio communications for green smart environments. [Available at http://www.ic1004.org/.]
IEEE Standard 802.15.4a-2007 (2007), Amendment to 802.15.4- 2006: Wireless Medium Access Control (MAC) and Physical Layer (PHY) Specifications for Low-Rate Wireless Personal Area Networks (LR-WPANs).
IEEE Std 802.15.6-2012 (2012), Wireless body area networks, 1 –271, February 2012.
Jovanov, E., A. Milenkovic, C. Otto, and P. C. De Groen (2005), A wireless body area network of intelligent motion sensors for computer assisted physical rehabilitation, *J. NeuroEngineering Rehabil.*, *2*(1), doi:10.1186/1743-0003-2-6.
Khan, I., P. Hall, Y. Nechayev, and L. Akhoondzadeh-Asl (2010), Multiple antenna systems for increasing on-body channel capacity and reducing ban-to-ban interference, International Workshop on Antenna Technology (iWAT).
Kim, M., and J. I. Takada (2009), Statistical model for 4.5 -GHz narrowband on-body propagation channel with specific actions, *IEEE Antennas Wirel. Propag. Lett.*, *8*, 1250–1254.
Kobayashi, T. (2009), Recent progress of ultra wideband radio propagation studies for body area network, 2nd International Symposium on Applied Sciences in Biomedical and Communication Technologies, 2009.
Kumpuniemi, T., T. Tuovinen, M. Hämäläinen, K. Y. Yazdandoost, R. Vuohtoniemi, and J. Iinatti (2013), Measurement-based on-body path loss modelling for UWB WBAN communications, 7th International Symposium on Medical Information and Communication Technology.
Lauzier, M., P. Ferrand, A. Fraboulet, H. Parvery, and J. Gorce (2013), Full mesh channel measurements on Body Area Networks under walking scenarios, 7th European Conference on Antennas and Propagation (EuCAP), 3508-3512, April 2013.
Li, X., and S. C. Hagness (2001), A confocal microwave imaging algorithm for breast cancer detection, *IEEE Microwave Wireless Compon. Lett.*, *11*(3), 130–132.
Liu, L., R. D'Errico, L. Ouvry, P. De Doncker, and C. Oestges (2011), Dynamic channel modeling at 2.4 GHz for on-body area networks, Advances in Electronics and Telecommunications - Radio Communication Series: Recent Advances in Wireless Communication Networks, 2(4).
Liu, L., S. van Roy, F. Quitin, P. De Doncker, and C. Oestges (2013), Statistical characterization and modeling of doppler spectrum in dynamic on-body channels, *IEEE Antennas Wirel. Propag. Lett.*, *12*, 186–189.
Mackowiak, M., and L. M. Correia (2011), Modelling the influence of body dynamics on the radiation pattern of wearable antennas in Off-body radio channels, in Proc. of 12th URSI Commission F Triennial Open Symposium on Radio Wave Propagation and Remote Sensing, Garmisch-Partenkirchen, Germany, Mar. 2011.
Mackowiak, M., C. Oliveira, and L. M. Correia (2012), Radiation pattern of wearable antennas: A statistical analysis of the influence of the human body, *Int. J. Wireless Inf. Networks*, *19*(3), 209–218.
Mackowiak, M., R. Rosini, R. D'Errico, and L. M. Correia (2013), Comparing off-body dynamic channel model with real-time measurements, 7th International Symposium on Medical Information and Communication Technology (ISMICT) 2013, Japan, 2013.
Maman, M., F. Dehmas, R. D'Errico, and L. Ouvry (2009), Evaluating a TDMA MAC for body area networks using a space-time dependent channel model, IEEE 20th International Symposium on Personal, Indoor and Mobile Radio Communications, 2101–2105, 13–16 Sept.
Miniutti, D., L. Hanlen, D. Smith, A. Zhang, D. Lewis, D. Rodda, and B. Gilbert (2008), Narrowband channel characterization for body area network, IEEE 802.15-08-0421-00-0006, July 2008.
Molisch, A. F., D. Cassioli, C. Chong, S. Emami, A. Fort, B. Kannan, J. Karedal, J. Kunish, and H. G. Schantz (2006), A comprehensive standardized model for ultrawideband propagation channels, *IEEE Trans. Antennas Propag.*, *54*(11), 3151–3166.
Mrozowski, M., and M. A. Stuchly (1997), Parameterization of media dispersive properties for FDTD, *IEEE Trans. Antennas Propag.*, *45*(9), 1438–1439.
Nechayev, Y. I., Z. H. Hu, and P. S. Hall (2009), Short-term and long-term fading of on-body transmission channels at 2.45 GHz, Loughborough Antennas & and Propagation Conference (LAPC), 657–660, 2009.
Oliveira, C., and L. M. Correia (2010), A statistical model to characterize user influence in body area networks, IEEE Vehicular Technology Conference Fall (VTC), September 2010.
Pedersen, G. F., J. Nielsen, O. Franek, J. B. Andersen, M. Pelosi, and Y. Wang (2009), Measurement based investigations for future communication system performance evaluation, Loughborough Antennas & Propagation Conference (LAPC).
Reusens, E., W. Joseph, G. Vermeeren, L. Martens, B. Latre, I. Moerman, B. Braem, and C. Blondia (2007), Path loss models for wireless communication channel along arm and torso: Measurements and simulations, IEEE Antennas and Propagation Society International Symposium, 345–348.
Rice, S. O. (1948), Statistical properties of a sine wave plus random noise, *Bell Syst. Tech. J.*, *27*, 109–157.
Roelens, L., S. Van den Bulcke, W. Joseph, G. Vermeeren, and L. Martens (2006), Path loss model for wireless narrowband communication above flat phantom, *Electron. Lett.*, *42*(1), 10–11.
Rosini, R., and R. D'Errico (2012a), Comparing On-Body dynamic channels for two antenna designs, Loughborough Antennas and Propagation Conference (LAPC), Nov. 2012.
Rosini, R., and R. D'Errico (2012b), Off-body channel modelling at 2.45 GHz for two different antennas, 2012 6th European Conference on Antennas and Propagation (EUCAP), 3378–3382.
Rosini, R., and R. D'Errico (2013), Space-time correlation for on-to-Off body channels at 2.45 GHz, European Conference in Antenna and Propagation 2013 (EuCAP 2013), Gothenburg, Sweden.
Rosini, R., R. D'Errico, and R. Verdone (2012), Body-to-body communications: A measurement–based channel model at 2.45 GHz, IEEE 23rd International Symposium on Personal Indoor and Mobile Radio Communications (PIMRC), 1763–1768.
Ryckaert, J., P. De Doncker, R. Meys, A. de Le Hoye, and S. Donnay (2004), Channel model for wireless communication around human body, *Electron. Lett.*, *40*(9), 543–544.


©2014. The Authors.

Salonen, P., Y. Rahmat-Samii, and M. Kivikoski (2004), Wearable antennas in the vicinity of human body, IEEE Antennas and Propagation Society International Symposium, 467–470.
Sanz-Izquierdo, B., F. Huang, and J. C. Batchelor (2006), Covert dual-band wearable button antenna, *IEE Electron. Lett.*, *42*(12), 3–4.
Sawada, H., T. Aoyagi, J. Takada, K. Y. Yazdandoost, and R. Kohno (2008), Channel model between body surface and wireless access point for UWB band, IEEE 802.15-08-0576-00-0006, August 2008.
See, T. S. P., J. Y. Hee, C. T. Ong, L. C. Ong, and Z. N. Chen (2009), Inter-Body channel model for UWB communications, 3rd European Conference on Antennas and Propagation, EuCAP 2009, March 2009.
Smith, D. B., and D. Miniutti (2012), Cooperative body-area-communications: First and second order statistics with decode-and-forward, IEEE Wireless Communications and Networking Conference (WCNC).
Smith, D. B., et al. (2009a), Temporal correlation of dynamic on-body area radio channel, *Electron. Lett.*, *45*(25), 1212–1213.
Smith, D., L. Hanlen, J. A. Zhang, D. Minutti, D. Rodda, and B. Gilbert (2009b), Characterization of the dynamic narrowband on-body to Off-body area channel, IEEE International Conference on Communications.
Smith, D., D. Miniutti, T. Lamahewa, and L. Hanlen (2013), Propagation models for body area networks: A survey and New outlook, *IEEE Antennas Propag. Mag.*, *55*(5), 97–117.
Stüber, G. L. (2011), *Principles of Mobile Communication*, 3rd ed., Springer.
Taparugssanagorn, A., C. Pomalaza-Raez, A. Isola, R. Tesi, M. Hämäläinen, and J. Iinatti (2010a), UWB channel modelling for wireless body area networks in a hospital, *Int. J. Ultra Wideband Commun. Syst.*, *1*(4), 226–236.
Taparugssanagorn, A., B. Zhen, R. Tesi, M. Hämäläinen, J. Iinatti, and R. Kohno (2010b), A Dynamic channel model of UWB-WBAN for some medical applications, 4th International Symposium on Medical Information and Communications Technology.
Tiberi, G., N. Ghavami, D. J. Edwards, and A. Monorchio (2012), UWB body area network channel modeling: An analytical approach, *Int. J. Electron. Commun. (AEÜ)*, *66*, 913–919.
Tsouri, G. R., A. Sapio, and J. Wilczewski (2011), An investigation into relaying of creeping waves for reliable low-power body sensor networking, *IEEE Trans. Biomed. Circuits Syst.*, *5*(4), 307–319.
van Roy, S., C. Oestges, F. Horlin, and P. De Doncker (2010), A comprehensive channel model for UWB multi-sensor multi-antenna body area networks, *IEEE Trans. Antennas Propag.*, *58*(1), 163–170.
van Roy, S., F. Quitin, L. Liu, C. Oestges, F. Horlin, J. Dricot, and P. De Doncker (2013), Dynamic channel modeling for multi-sensor body area networks, *IEEE Trans. Antennas Propag.*, *61*(4), 2200–2208.
Van Torre, P., L. Vallozzi, L. Jacobs, H. Rogier, M. Moeneclaey, and J. Verhaevert (2012), Characterization of measured indoor off-body MIMO channels with correlated fading, correlated shadowing and constant path loss, *IEEE Trans. Wireless Commun.*, *11*(2), 712–721.
Viittala, H., M. Hamalainen, J. Iinatti, and A. Taparugssanagorn (2009), Different experimental WBAN channel models and IEEE802.15.6 models: Comparison and effects, 2nd International Symposium on Applied Sciences in Biomedical and Communication Technologies.
Wang, Y., I. B. Bonev, J. O. Nielsen, I. Z. Kovacs, and G. F. Pedersen (2009), Characterization of the indoor multiantenna body-to-body radio channel, *IEEE Trans. Antennas Propag.*, *57*(4), 972–979.
Wong, K. L., and C. I. Lin (2005), Characteristics of a 2.4-GHz compact shorted patch antenna in close proximity to a lossy medium, *Microwave Opt. Technol. Lett.*, *45*(6), 480–483.
Wuren, T., T. Takai, M. Fujii, and I. Sakagami (2007), Effective 2-Debye-pole FDTD model of electromagnetic interaction between whole human body and UWB radiation, *IEEE Microwave Wireless Compon. Lett.*, *17*(7), 483–485.
Yacoub, M. D. (2007), The $\alpha$-$\mu$ distribution: A physical fading model for the Stacy distribution, *IEEE Trans. Veh. Technol.*, *56*(1), 27–34.
Yacoub, M. D., J. E. V. Bautistu, and L. Guerra de Rezende Guedes (1999), On higher order statistics of the Nakagami-*m* distribution, *IEEE Trans. Veh. Technol.*, *48*, 790–794.
Yacoub, M. D., D. B. da Costa, U. S. Dias, and G. Fraidenraich (2005), Joint statistics for two correlated Weibull variates, *IEEE Antennas Wirel. Propag. Lett.*, *4*, 129–132.
Yazdandoost, K., and K. Sayrafian-Pour (2010), Channel model for body area network (BAN), IEEE p802.15-08-0780-12-0006, November 2010.
Zasowski, T., F. Althaus, M. Stager, A. Wittneben, and G. Troster (2003), UWB for noninvasive wireless body area networks: Channel measurements and results, IEEE Conference on Ultra Wideband Systems and Technologies.
Zhang, A. J., L. W. Hanlen, D. Minutti, D. Rodda, and B. Gilbert (2009), Interference in Body Area Networks: Are signal-links and interferece-links independent? 2009 IEEE 20th International Symposium on Personal, Indoor and Mobile Radio Communications.
Ziri-Castro, K. I., W. G. Scanlon, and N. E. Evans (2004), Indoor radio channel characterization and modeling for a 5.2 GHz bodyworn receiver, *IEEE Antennas Wirel. Propag. Lett.*, *3*(1), 219–222.


©2014. The Authors.